NUREG/CR-3742
LA-10087-MS

Los Alamos National Laboratory is operated by the University of California for the United States Department of Energy under contract W-7405-ENG-36

Buckling of Steel Containment Shells Under Time-Dependent Loading

Los Alamos
Los Alamos National Laboratory
Los Alamos, New Mexico 87545

NUREG/CR-3742
LA-10087-MS

R5

Buckling of Steel Containment Shells Under Time-Dependent Loading

C. D. Babcock*
W. E. Baker**
J. Fly
J. G. Bennett

Manuscript submitted: March 1984
Date published: May 1984

Prepared for
Mechanical/Structural Engineering Branch
Division of Engineering Technology
Office of Nuclear Regulatory Research
US Nuclear Regulatory Commission
Washington, DC 20555

NRC FIN No. A7221

*Consultant at Los Alamos. California Institute of Technology, Pasadena, CA 91125.
**Collaborator at Los Alamos. University of New Mexico, Albuquerque, NM 87131.

Los Alamos Los Alamos National Laboratory
Los Alamos, New Mexico 87545

CONTENTS

FIGURES

U. S. Nuclear Regulatory Commission

Reports in Buckling Research Series

An Investigation of Buckling os Steel Cylinders in Circular Cutouts Reinforced in Accordance with ASME Rules, J. G. Bennett, R. C. Dove, T. A. Butler, Los Alamos Scientific Laboratory report LA-8853-MS, NUREG/CR-2165, June 1981.

Buckling Investigation of Ring-Stiffened Cylindrical Shells Under Unsymmetrical Axial Loads, William Baker, Joel Bennett, Charles Babcock, Los Alamos National Laboratory report LA-9536-MS, NUREG/CR-2966, October 1982.

Buckling Investigation on Ring-Stiffened Cylindrical Shells with Reinforced Openings under Unsymmetrical Axial Loads, William Baker, Joel Bennett, Los Alamos National Laboratory report LA-9646-MS, NUREG/CR-3135, February 1983.

BUCKLING OF STEEL CONTAINMENT SHELLS UNDER TIME-DEPENDENT LOADING

by

C. D. Babcock, W. E. Baker, J. Fly, and J. G. Bennett

ABSTRACT

The problem of dynamic effects for steel containment shells subjected to time-dependent loadings that produce large compressive membrane stresses in the shell wall is considered. Loadings on typical containment structures are reviewed, along with a description of the complete dynamic-buckling problem. Simplifications and the assumptions that are currently used are critically examined and reviewed with respect to buckling analysis. Based on these reviews, three program objectives are defined and the tasks that can accomplish these objectives within a 2-year effort at level funding are outlined in detail.

I. INTRODUCTION

Nuclear steel containments are analyzed for a wide variety of postulated loadings and load combinations. In reality, with the exception of gravity loadings, all of these loadings are time varying, but when the time scale for this variation is compared with structural or thermal response time for the containment, many of them can be treated in a static or quasi-static manner. We will discuss the time-scale effects with respect to the dynamic-buckling problem fully in Sec. II.

The problem addressed by this program is the buckling of typical nuclear steel containment vessels under true dynamic loadings. These loadings must be characterized in terms of the loading time as compared with the assumed buckling response mode and duration to determine if dynamic buckling is a consideration; if not, perhaps conventional static-buckling procedures may be applied. Any loading capable of producing large compressive membrane stresses must be considered; the ones considered here fall into two broad categories. These categories are the loss-of-coolant accidents (LOCA) and seismic loading. There are three types of loadings that produce large thermal and direct asymmetric pressure inside the containment: (a) anticipated transient without scram (ATWS), (b) large pipe break and whip, and (c) ice condenser pressure transients.

Seismic loadings must also be considered as capable of producing buckling failure. In both design analyses and safety analyses, combinations involving seismic loadings and LOCA loadings are generally accounted for by some method of superposition of the loadings. To date however, there has been little or no uniformity in treatment of buckling caused by dynamic response. The generally used analysis technique is the freezing-in-time method, which is discussed fully in Sec. II.

In Sec. III we discuss the three objectives developed for this program and the orderly approach appropriate for achieving these objectives.

Section IV describes in detail the technical tasks we will perform to achieve the program objectives: an analysis task, a scaling-law analysis task, a Lexan-model experimental task, and a bench mark experimental task on steel models.

Finally, in Sec. V we summarize the dynamic-buckling program and make recommendations on other supporting efforts that can and may be included if funding allows.

II. PRESENT DESIGN/ANALYSIS PROCEDURES

A. Analysis Criteria

The loading conditions described in Sec. I produce time-dependent displacements and stresses in the containment shell structure; these stresses and displacements usually have a complex spatial dependence that changes as a function of time. To ensure the adequacy of the containment shell design, allowable stresses and/or displacements must be compared with the calculated quantities.

If the failure condition is based upon an allowable stress (or a combination of stresses), the calculated stresses can be compared directly with the allowable ones. This procedure appears to be a straightforward matter, but its implementation is difficult because of large amounts of data generated by any dynamic stress analysis. In addition, judgment must be exercised as to which calculated stresses are real and which result from modeling inadequacies. Modeling problems always exist in analysis of complex structures because of the economic infeasibility of modeling all structural details.

If the failure condition is based upon an allowable displacement, again a direct comparison of calculated and allowable displacement can be made. The concept of dynamic buckling (that is, buckling under dynamic loading conditions) does not fit neatly into this description of failure conditions. This misfit results because dynamic buckling is actually just some combination of unacceptably large stresses and/or displacements (a "dynamic-buckling criterion") that results from a time-dependent loading. However, the dynamic buckling calculations are rarely carried out in this manner. Usually, the analyst attempts to relate the calculated dynamic stresses to some static buckling criterion to produce a "dynamic buckling load;" However, the rationale behind this procedure is largely unexplored and usually not adequately understood by the analyst.

This analysis procedure is commonly referred to as the "freezing-in-time" technique. The name results from the time-dependent stresses that are assumed to be static (frozen in time) during performance of the buckling analysis. This procedure assumes implicitly that the stress field that causes the buckling changes very little during the time it takes the structure to buckle.

The steps in this type of analysis vary from investigation to investigation. The transient response is usually determined using a linear analysis. The analysis could be nonlinear (both geometric and material), but geometric nonlinearities probably have little effect; a shallow sperical cap under transient pressure is a noteworthy exception. Material nonlinearity (plasticity) has not been investigated to any extent for this type of problem; realistic edge conditions, discrete stiffeners, cutouts, attached equipment, etc., can be included in the transient analysis depending on the degree of complexity (and computer costs) the analyst is willing to deal with.

The next step in the analysis may be carried out in a variety of manners. The simplest way is to choose an appropriate moment in time using engineering judgment and locate the area of largest membrane stresses. These stresses are assumed to act over the complete shell. The buckling condition is then found from a closed form solution, empirical formula, or numerical computation.

Another variation is to use the complete spatial distribution of membrane stresses from the transient analysis and perform a bifurcation analysis; this method usually necessitates the use of a computerized shell analysis. A further refinement would include prebuckling bending stresses in the bifurcation analysis. The buckling analysis should be carried out for a number of different times to assure that the worst instance has been chosen.

It is surprising that this method of analysis has gained acceptance without available evidence to verify its accuracy and to assess the limits of applicability. Perhaps the ready acceptance results because all actual buckling (laboratory or field) is caused by transient loads. In the laboratory, the load on a shell is slowly increased until buckling occurs. The key feature is the loading time scale as compared with the buckling time scale. This fact is seldom pointed out in buckling experiments but is subconsciously addressed by the experimenter when applying the load. In the freezing-in-time analysis, the separation of the time scales is not addressed but is usually assumed to exist. Consequently, the time scales need to be studied in more detail if the situation is to be quantified.

The time scale usually associated with buckling is that of the period of the buckling mode. While there is not a one-to-one relation between a buckling mode and a vibration mode, they are quite similar in shape (identical in some simple cases). Meller and Bushnell (Ref. 1) have studied one containment shell in detail; Fig. 1 shows the details of the shell, assumed to be axisymmetric. The natural frequencies and mode shapes, calculated using BOSOR 4, are shown in Fig. 2; frequencies are identified by mode shape. The lowest shell-type modes correspond to the cylindrical shell vibrating like an orthotropic shell with the axial and circumferential stiffeners deforming with the shell skin. The sphere modes are easily identifiable as are the interbay modes (vibration between rings).

The lowest frequency for this containment shell is 6.4 Hz and corresponds to five full-circumferential waves with a half wave in the axial direction. There are 12 of these types of modes with frequencies below 15 Hz. Which mode correponds to the buckling mode is not clear as neither a full dynamic-buckling analysis nor a model experiment has been carried out. If the buckling were dominated by shear, then a single-half wave in the axial direction with a number of circumferential waves would be expected. Axial-stress-dominated buckling would produce several waves in the axial direction. A rough

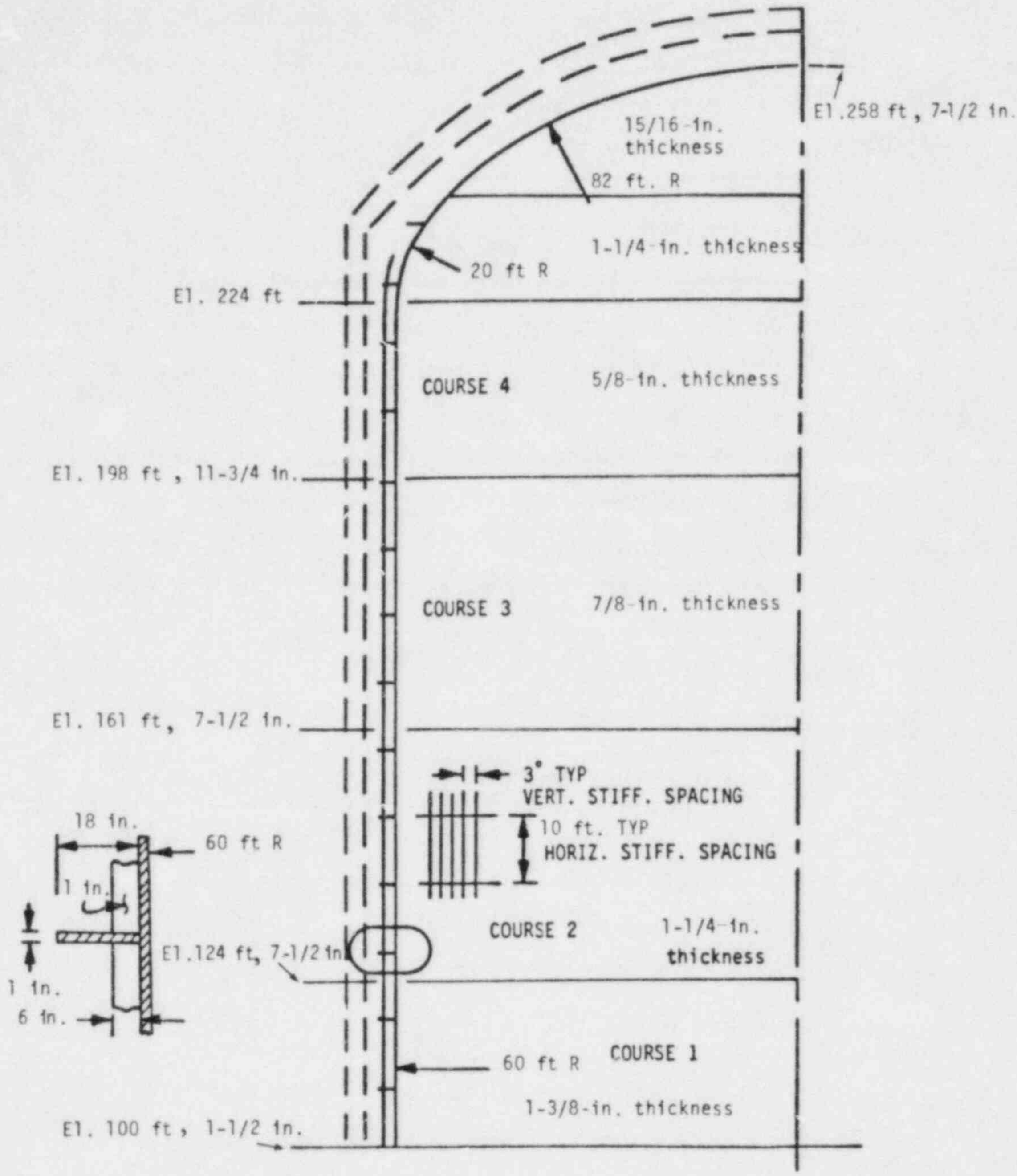

Fig. 1. Offshore Power Systems containment shell studied by Meller and Bushnell (Ref. 1).

estimate of the buckling response time can be made from this type of data. For the Offshore Power Systems (OPS) containment shell, this estimate would be

$$T_{bu} \sim 0.05 \text{ to } 0.15 \text{ s.}$$

The other time scale in the dynamic-buckling problem is one corresponding to the transient stress in the shell structure; the stress field in turn depends upon the loading and the important response modes. For the seismic-loading problem, the important response modes are the "beam type" modes of the shell (n=1). From Fig. 2, note that the first two of these modes have frequencies of 8.5 Hz and 22.7 Hz. The response in these modes can be found using the NRC Regulatory Guide 1.60 (Ref. 2) for seismic analysis. The horizontal design response spectra are shown in Fig. 3. The lower mode (8.5 Hz) is in the range of frequencies where considerable amplification is expected. However, the next frequency (22.7 Hz) is outside the range of significant response amplification and will probably contribute little to the dynamic response.

For the seismic-response problem, it is then expected that the predominate response will be at 8.5 Hz. This response time (T_{re} = 0.12 s) is close to the expected time of buckling. This coincidence of buckling and response time implies that the assumptions of the freezing-in-time technique may not be valid or at least that the results of such an analysis should be validated by dynamic-buckling experiments.

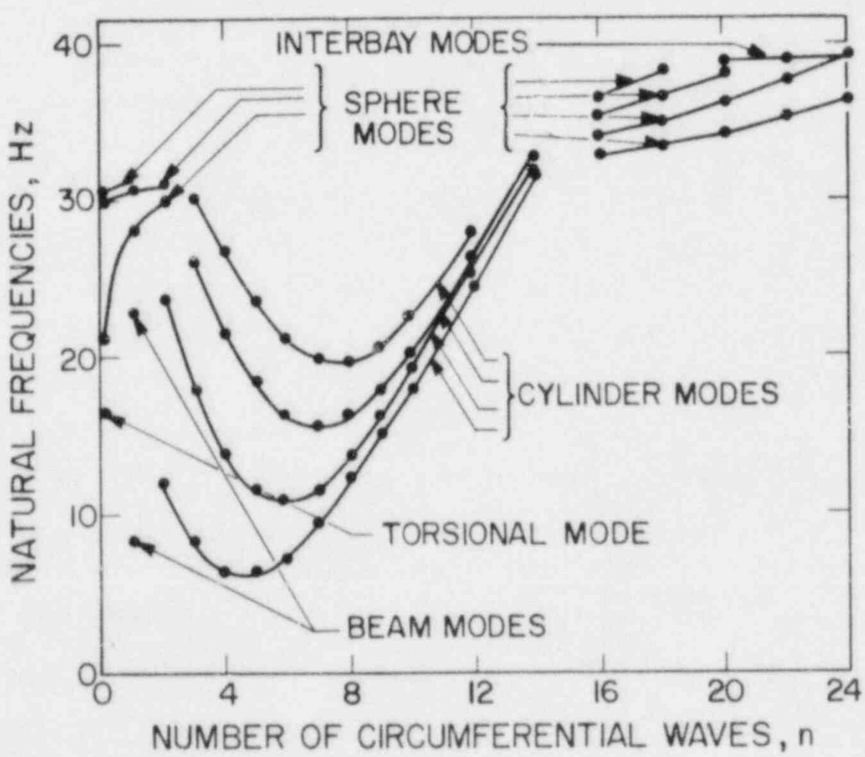

Fig. 2. Natural frequencies and corresponding modes of OPS containment shell.

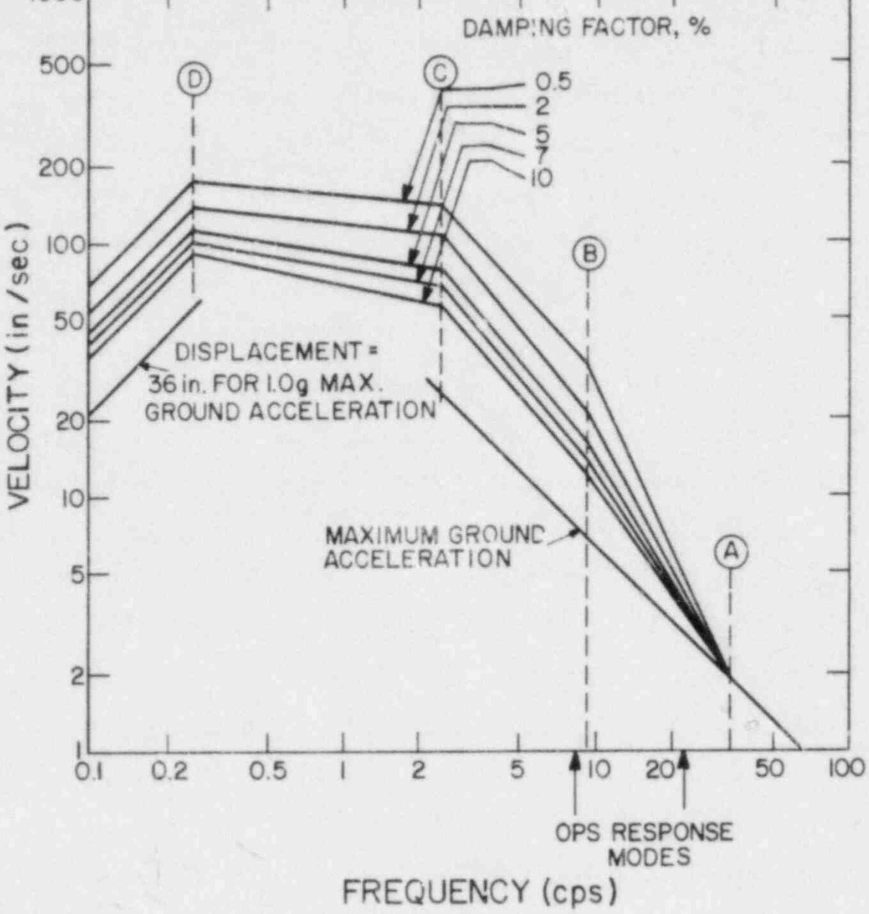

Fig. 3. Horizontal design response spectra--scaled to 1-g horizontal ground acceleration.

B. Other Considerations

Damping affects both the primary dynamic response and the buckling response; however, in the procedure described above, the effect of damping has not been discussed. For the primary response, the damping effect is shown on the design response spectra (Fig. 3). The damping value specified by Ref. 2 for welded steel structures is either 2% or 4% (per cent critical damping), depending upon the seismic event being studied. The difference in response of the fundamental mode is approximately 20%, depending on the value used.

The damping can also affect the buckling behavior. If buckling occurs in a monotonic manner (such as the static case), damping would appear to have little effect. However, if there is coupling between the response and buckling modes (such as a parametric resonance), damping can play an important role. Its value can be the predominant factor in determining stability.

C. Load Interaction

The technique described above for finding the dynamic-buckling load requires the solution of a static-buckling problem. The prebuckling stress state is that derived from the dynamic stress analysis and, in general, is quite complex in its spatial distribution. There are several approximations that can be made to simplify this task. One approximation is to assume that the stresses are uniform throughout the shell structure, their value being the maximum at any specific time. This assumption allows a simple interaction-buckling equation (for example, shear and axial compression) to be used to determine the allowable buckling stress. However, this simplification may lead to very conservative results if the high stresses in the shell are localized. Another method is to perform a linearized bifurcation analysis using the complete shell stress distribution at any point in time. This method can be quite costly because the resulting eigenvalue problem will be very large if the shell structure is properly modeled.

A third procedure is to use experimental results for the buckling-interaction criterion. If the same shell is used for this test as well as for the dynamic-buckling tests, the knockdown factor resulting from imperfections is automatically incorporated into the results. The difficulty associated with the procedure is duplicating, in an appropriate manner, the dynamically induced stress field by a static-loading method. The static-prebuckling stress field should model the important features of the dynamic stress field.

III. PROGRAM OBJECTIVES

Based on the material we reviewed in arriving at the descriptions and analyses presented in Secs. I and II, three program objectives have been formulated for this dynamic-buckling study. These objectives are as follows:

1. assess the adequacy of current (and past) design and analysis procedures for the prevention of buckling of containment vessels under time-dependent loadings,
2. carry out bench mark experiments (that will provide the information necessary to validate analysis procedures) on typical containment-like models subjected to scaled dynamic loadings, and

3. carry out experiments whose main objectives are to assess the postbuckling behavior of a typical containment vessel and the consequences of this behavior on the potential for loss of containment.

This program will achieve these objectives using a combined analytical/experimental approach that will proceed in an orderly fashion from the simpler models and loadings to the more complex.

There are a number of significant problems to be addressed in achieving these objectives, including an assessment of the assumptions that are usually made in analysis of dynamic buckling. Some of these assumptions may simply be physically incorrect, such as the assumption that the buckling mode responds like the vibration mode that it most resembles in deformation. Reference 3 cites some evidence that this assumption is incorrect. Other assumptions, such as the one always implicitly made regarding time-scale separation that $T_{BU} << T_{Loading}$, are known to be incorrect for certain loadings.[3] The magnitude of the error of making this assumption must be addressed. If, in certain loading situations, there proves to be a significant dynamic effect and a dynamic-buckling criteria is needed, questions such as, "Which one should be applied?" and, "How is it to be determined?" must be answered.

Other problems that must be solved are primarily in the postbuckling response area. These problems include both validation problems associated with nonlinear predictive codes that can compute the postbuckling behavior and the very difficult problems of defining material failure criteria in terms of ductile tearing or weldment failure that will define loss of containment. Note that, while there is currently a significant amount of research being carried out on ductile crack initiation and extension that may be of use here, no concensus has been reached among various researchers on the best descriptive analytical models and their limits.

The technical tasks discussed in Sec. IV (to achieve the program objectives) have been planned with these and other problems identified; performing these tasks will either solve or redefine the problems in an orderly fashion.

IV. TECHNICAL TASKS

The technical tasks designed to achieve the program objectives are designed to accommodate an increasing order of complexity as the experimental/analytical work proceeds. Each task interfaces with the others, but the experimental tasks are generally related to each other through the analysis task.

A. Analysis Task

The analysis tools to be employed are the following numerical computer codes:

1. SABOR/DRASTIC 7 (Ref. 4),
2. BOSOR 4 (Ref. 5),
3. BOSOR 5 (Ref. 6),
4. SPAR (Ref. 7), and
5. ABAQUS (Ref. 8).

The first two are axisymmetric codes that make use of the combined numerical semianalytical process of describing the loading as a Fourier series. If the geometry and material properties do not vary with the circumferential coordinate, the analysis of the three-dimensional loadings can be performed using the axisymmetric codes by superposition of the results from each harmonic to synthesize the three-dimensional result. In this method, if (X_1, X_2, X_3) are coordinates describing the domain and, for the $(0 \leq X_3 \leq a)$ coordinate, the geometry and material properties do not change, then all variations in X_3 of stresses and displacements can be expanded in a Fourier series. Regardless of the method of discretization, the matrix equations governing the undamped structural response can be written in the form

$$[M]\{\ddot{z}\} + [K]\{z\} = \{F(t)\} , \tag{1}$$

where $[M]$ = the mass matrix,
$[K]$ = the stiffness matrix,
$\{z\}$ = the displacement vector for the discretized coordinates, and
$\{\ddot{z}\}$ = the acceleration vector.

With the loads, displacements, and stresses expanded in a series of orthogonal functions, the terms in the stiffness matrix, [K], will involve integrals of products of orthogonal functions, and the large system of equations will uncouple into "L" separate problems, where L is the truncated number of terms in series expansion.

This procedure has great practical application, particularly if the loading function can be described using a minimum number of terms or if the analyst knows that a particular harmonic is the only important one. For example, the horizontal base acceleration, $\ddot{u}_g$, of a circular base steel containment can be adequately described as

$$\ddot{u}_g = a(t) \cos \theta \quad , \tag{2}$$

with a(t) the time-dependent amplitude, and θ the circumferential coordinate, and the dots indicating derivatives with respect to time, t. This description means we need only solve for the n=1 harmonic structural response to determine the stress resultants, N, that will be expressed as

$$\begin{aligned} N_s &= F_1(s,t) \cos \theta, \\ N_\theta &= F_2(s,t) \cos \theta, \\ N_{s\theta} &= F_3(s,t) \sin \theta, \end{aligned}$$

where s is the meridional coordinate.

For a rapid evaluation of the severity of the loading, combinations of N_s, N_θ, and $N_{s\theta}$ can then be displayed on static-buckling interaction curves as illustrated in Fig. 4. This method of evaluation is the basic procedure for the freezing-in-time method of analysis described in Sec. II.

In this program, typical containment shells will be modeled and loaded seismically in this manner and a postprocessor will be written to carry out the rapid evaluation of all stress resultants using such interaction curves. Both analytically developed interaction curves and experimentally determined curves will be used. The purpose of this step is to assess the severity of earthquake loading on typical containment structures.

A second use of the analytical models of these containments will be to estimate their structural natural frequencies as well as those of the experimental models. To evaluate the dynamic effects of a seismic excitation on the experimental models, it is important to ensure that the frequency spectrum of the experimentally applied excitation bears the same relationship to the containment-like model as the actual earthquake bears to the real containment. These relationships will be determined analytically so that proper time scaling of seismic signals can be carried out. The BOSOR 4 computer code will be the primary tool for obtaining the initial natural-frequency estimates.

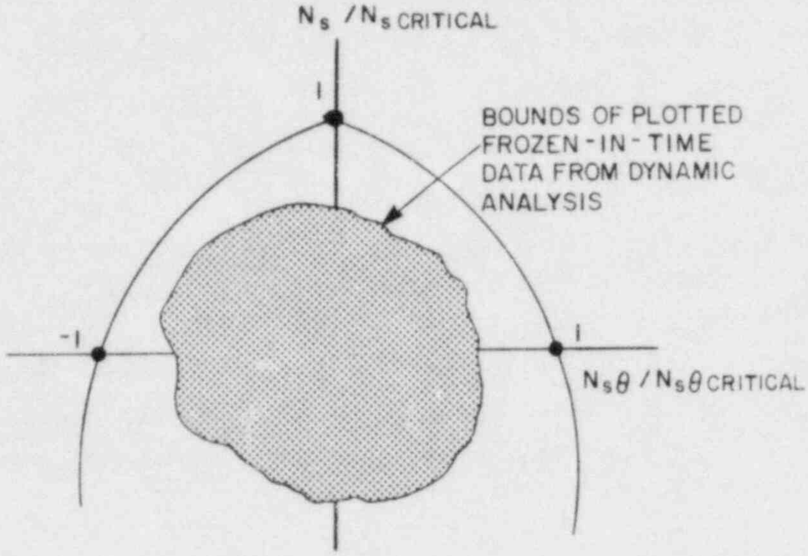

Fig. 4. Buckling interaction curve and rapid evaluation scheme for time-dependent stress resultants.

A comparison of the experimentally and analytically determined natural frequencies will also be used to assess the accuracy of the analytical models where appropriate.

For models that will require three-dimensional response evaluations, the computer codes SPAR and ABAQUS will be used. SPAR is very efficient for linear modeling and eigenvalue extraction, whereas ABAQUS is an effective nonlinear modeling tool and will be used primarily in the postbuckling response phase for evaluation of, and analytical support of, the experiments. BOSOR 5 will also be of use in this phase to determine axisymmetric plasticity effects.

Generally, the analytical task will support and guide all experiments as needed. Results of the experiments can then be interpreted for actual containments with confidence.

B. Model Design

The experimental studies to be accomplished for this investigation are intended to serve two functions. One of these functions is to furnish experimental results that may be used as a guide in the evaluation of dynamic-buckling analysis methods. The second function will be to determine characteristic dynamic response for steel containments attributable to seismic inputs from model tests with particular emphasis on stability. In the design of the experimental program, the models used to address the first function will have containment-like geometry, and the dynamic excitations used during the tests will include a seismic-type input representative of that which containments might see. The models used for the second phase of the experimental program will be scale models of a typical steel containment, designed and tested in accordance with appropriate scaling laws. In this section of the program plan, the scaling laws will be developed and preliminary information on the design of the models is presented.

The significant parameters and their dimensions in the force, length, time (FLT) system that should be included in a study of stability of steel containments to a dynamic excitation are as follows:

$\ddot{x}$ = acceleration, $[LT^{-2}]$;
g = acceleration of gravity, $[LT^{-2}]$;
ℓ = characteristic length, $[L]$;
t = time, $[T]$;
E = stress-strain material property, $[FL^{-2}]$;
ρ = density of material, $[FL^{-1}T^{2}]$;
F = force, $[F]$; and
σ = stress, $[FL^{-2}]$.

With the exception of g, each of the above parameters represents a characteristic quantity in the model study, and any specific feature will be identified with a subscript as required. The acceleration of gravity will not be modeled; it is explicitly identified to permit its inclusion in the analysis so that any distortion of gravity may be easily examined and the effect studied. It should also be pointed out that this list of parameters is based upon the assumption that the internal and external pressures acting on the containment vessel are equal and constant.

The governing equation for buckling in terms of these parameters will be written in terms of the buckling stress, σ_B, and will be of the form

$$\sigma_B = \phi\,(\ddot{x}, g, \ell, t, E, \rho, F, \sigma).$$

The nine parameters and three dimensions involved here (that is, F, L, T) may be expressed in terms of six groups of dimensionless variables in conformance with similitude theory. The relation, based upon one grouping of the variables involved, is as follows:

$$\left(\frac{\sigma_B}{E}\right) = d\left(\frac{\ddot{x}t^2}{\ell}, \ \frac{g}{\ddot{x}}, \ \frac{\rho\ell\ddot{x}}{E}, \ \frac{\sigma}{E}, \ \frac{F}{E\ell^2}\right) . \tag{3}$$

For an undistorted model and test conditions, the design conditions would be

$$\left(\frac{\ddot{x}t^2}{\ell}\right)_m = \left(\frac{\ddot{x}t^2}{\ell}\right)_p , \tag{4}$$

$$\left(\frac{g}{\ddot{x}}\right)_m = \left(\frac{g}{\ddot{x}}\right)_p , \tag{5}$$

$$\left(\frac{\rho\ell\ddot{x}}{E}\right)_m = \left(\frac{\rho\ell\ddot{x}}{E}\right)_p , \tag{6}$$

$$\left(\frac{\sigma}{E}\right)_m = \left(\frac{\sigma}{E}\right)_p , \tag{7}$$

$$\left(\frac{F}{E\ell^2}\right)_m = \left(\frac{F}{E\ell^2}\right)_p . \tag{8}$$

Here, the subscriptions "m" and "p" have been used to indicate the parameters associated with the model and the prototype, respectively. Geometric similarity is implied through the use of only one variable for length. The prediction equation for buckling of the prototype based upon measurements in the model would be

$$\left(\frac{\sigma_B}{E}\right)_p = \left(\frac{\sigma_B}{E}\right)_m . \tag{9}$$

The required scale factors for similarity may be derived from Eqs. (4) through (8). Here a scale factor, N_i, will be defined as the value of the "i" parameter in the model system divided by the value in the prototype system. Hence, the length scale, N_ℓ, is

$$N_\ell = \frac{\ell_m}{\ell_p} . \tag{10}$$

From Eq. (4),

$$N_t = \left[\left(\frac{\ddot{x}_p}{\ddot{x}_m}\right) \left(\frac{\ell_m}{\ell_p}\right)\right]^{1/2} . \tag{11}$$

From Eq. (5),

$$N_{\ddot{x}} = \frac{g_m}{g_p} . \tag{12}$$

From Eq. (6),

$$N_E = \left(\frac{\rho_m}{\rho_p}\right) \left(\frac{\ell_m}{\ell_p}\right) \left(\frac{\ddot{x}_m}{\ddot{x}_p}\right) . \tag{13}$$

From Eq. (7),

$$N_\sigma = \left(\frac{E_m}{E_p}\right) . \tag{14}$$

And finally, From Eq. (8),

$$N_F = \left(\frac{E_m}{E_p}\right) \left(\frac{\ell_m}{\ell_p}\right)^2 . \tag{15}$$

All of these scale factors would have to be satisfied for the model to be distortionless and the prediction Eq. (9) to apply. However, it is not practical to design and construct a model or to test it for conditions which are exactly scaled. For example, if the model is to be tested in a 1-g gravitational field, Eq. (12) requires the acceleration scale to be valued at 1.0; then Eq. (13) places impractical restriction on other scales. Therefore, for practical reasons, it will be necessary to consider that gravity is distorted during the model tests, and then to investigate the effects of this distortion on the validity of the results.

In the study of dynamic buckling of shells, one significant requirement is that the models constructed be reusable, at least during the development stages of the work. This requirement places certain restrictions on the selection of the material. The material selection, model details, and subsequent related analysis will be presented in the following sections.

C. Material Selection

As has been mentioned above, the experimental work in this program plan will support the validation of analysis methods for dynamic buckling of containment shells and will furnish information on characteristic response of containments to seismic input. These two different functions require different model materials.

The test results needed for the development of the analysis techniques will require that tests be conducted for several different types of loading conditions. Also, because seismic excitation is vibratory in nature, one load condition could result in a model being buckled several times. The high cost of models requires that the models used in this phase of the work be constructed of a material that can be buckled many times with essentially the same response. Because buckling of metal models normally results in deformation of the shell into the inelastic range and causes permanent deformation, materials other than metal must be used.

Plastics have been used for many studies of buckling, both static and dynamic, and these investigations have been reviewed by Babcock (Ref. 9) in some detail. The important factor is that certain plastics have the property of remaining perfectly elastic through reasonable postbuckling deformations, and consequently may be subject to buckling deformations numerous times without substantial degradation of buckling strength.

Preliminary work has been done on two types of plastic commonly used in buckling work: a polyester (Mylar) and polycarbonate (Lexan). For each of these materials, several cylindrical shells having an R/t ratio of about 460 were constructed and tested in axial compression. Both of the materials met the requirements of repeated buckling with essentially no degradation of buckling strength. However, model construction with the polycarbonate material is simpler and more reliable, primarily because solvent bonding can be used. Also, the range of stock sizes for the polycarbonate material is much greater than for Mylar; this feature gives greater flexibility in the model design and further simplifies model construction. The polycarbonate has been selected for use as the plastic model material for this phase of the work.

The experimental models used to determine characteristic containment response will be made of an A516 steel commonly used in containments. The buckling problem of particular interest here would involve material deformations into the inelastic and plastic range; similitude would require that the model and prototype materials have the same stress-strain curve in the range covering the deformations encountered in the prototype response. The only practical way to accomplish this requirment is to use the same material.

D. Plastic Models

The plastic models will be open-ended cylindrical shells for which the shell components will basically model a Mark III steel containment. Geometrical features to be modeled include the following:

1. radius-to-wall-thickness ratio,
2. radius-to-height ratio, and
3. ring-stiffener geometry (the area and section modulus designed to satisfy the American Society of Mechanical Engineers (ASME) code requirements.)

The variable wall thickness will not be modeled, and there will be no penetrations or related reinforcement.

Some preliminary work has been done on this phase of the project. The work completed includes development of fabrication methods for the polycarbonate models and some test work on the material and the models.

Two types of tests have been conducted on the material to determine the stress-strain relation. One type of test was the simple tension test on dumbbell-type specimens. Because the rate of strain may affect the stress-strain curve in the range of strain rates encountered in this work, these tests were run at several rates. To further study the magnitude of the strain-rate effect, tests were run using a vibrating cantilever beam of Lexan, and the modulus of elasticity was calculated from measured natural frequencies.

The tension tests were run on two thicknesses of stock, 0.015 in. and 0.067 in., for specimens that would be oriented both axially and circumferentially in a cylindrical model, and at strain rates to 0.67/min. The tests were run on a mechanical-drive testing machine. Figure 5 shows some results of these tension tests.

The tests on the clamped-free vibrating beam were made on a specimen 0.06 in. thick. The natural frequency of the beam was varied by changing the effective length (that is, the length measured from the clamped end), and the frequency range from 20 to 250 Hz was covered. The natural frequency was measured with an optical pickup. The elastic modulus was calculated from an equation for the first mode natural frequency. The results did not show a distinct strain-rate effect; in fact, the elastic moduli calculated by this method were slightly less than the values shown on Fig. 5.

A model construction technique has been developed for the polycarbonate models that results in good quality models at reasonable cost. The details of the process will not be given here, except to mention that the construction process is based on solvent bonding of the polycarbonate parts and potting the ends of the shell in a casting epoxy. Figure 6 shows a completed ring-stiffened shell that is still in the end forms that served as molds for the casting process; the threaded rods hold the end forms in proper alignment.

While the polycarbonate models will be used primarily in the validation of analysis techniques, these models will have features representative of containments and the test conditions will also be based upon the appropriate scale factors. Consequently, a discussion of scaling of the plastic models is appropriate here.

It is helpful to return to the earlier scaling discussion and to look in greater detail at a necessary distortion in the models. An initial analysis indicates that a distortion of gravity may be the least undesirable and the type of distortion most easily compensated for or understood.

As mentioned above, the acceleration scale, Eq. (12), is the one that places difficult restrictions on material properties of the model. The case

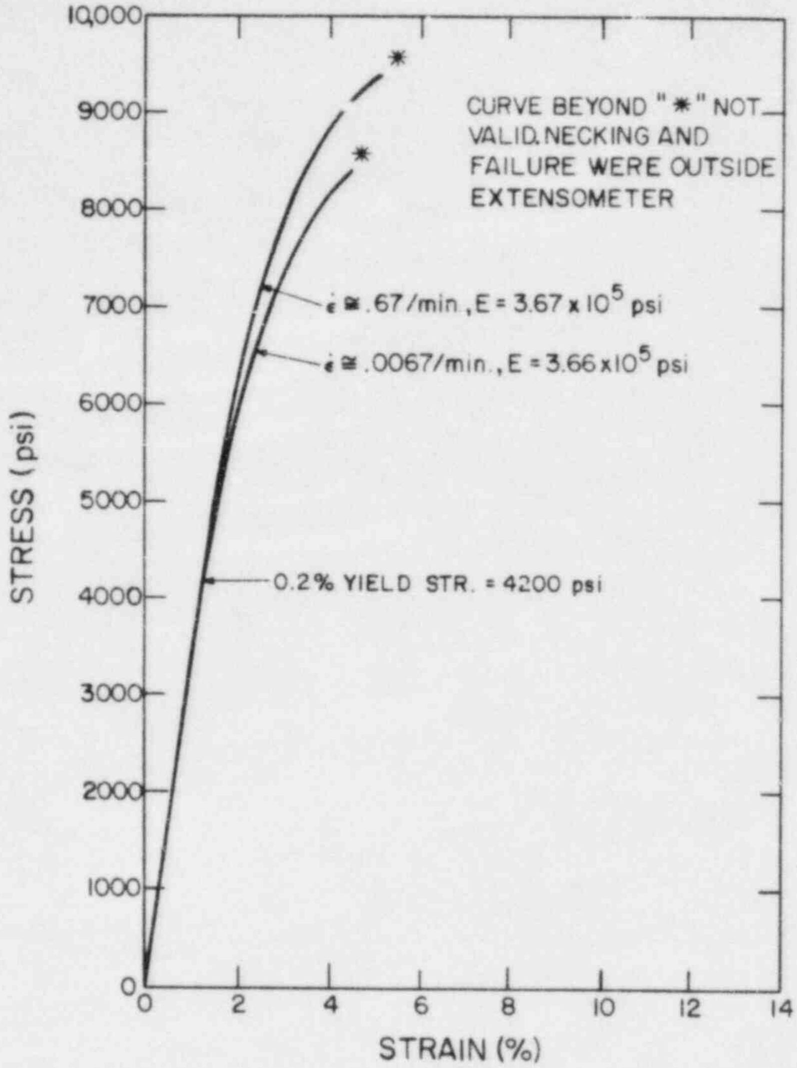

Fig. 5. Stress-strain curves for 1.52-mm-(0.060-in.-) thick Lexan.

where gravity is distorted $N_{\ddot{x}} = 1$ will be considered. The length scale and elastic modulus scale will be selected based on other considerations so that N_{ℓ} and N_E are specified. This selection also specifies the density scale, N_{ρ}. The acceleration scale may then be determined from Eq. (13) as

$$N_{\ddot{x}} = \frac{N_E}{N_{\rho}\, N_{\ell}} \quad . \tag{16}$$

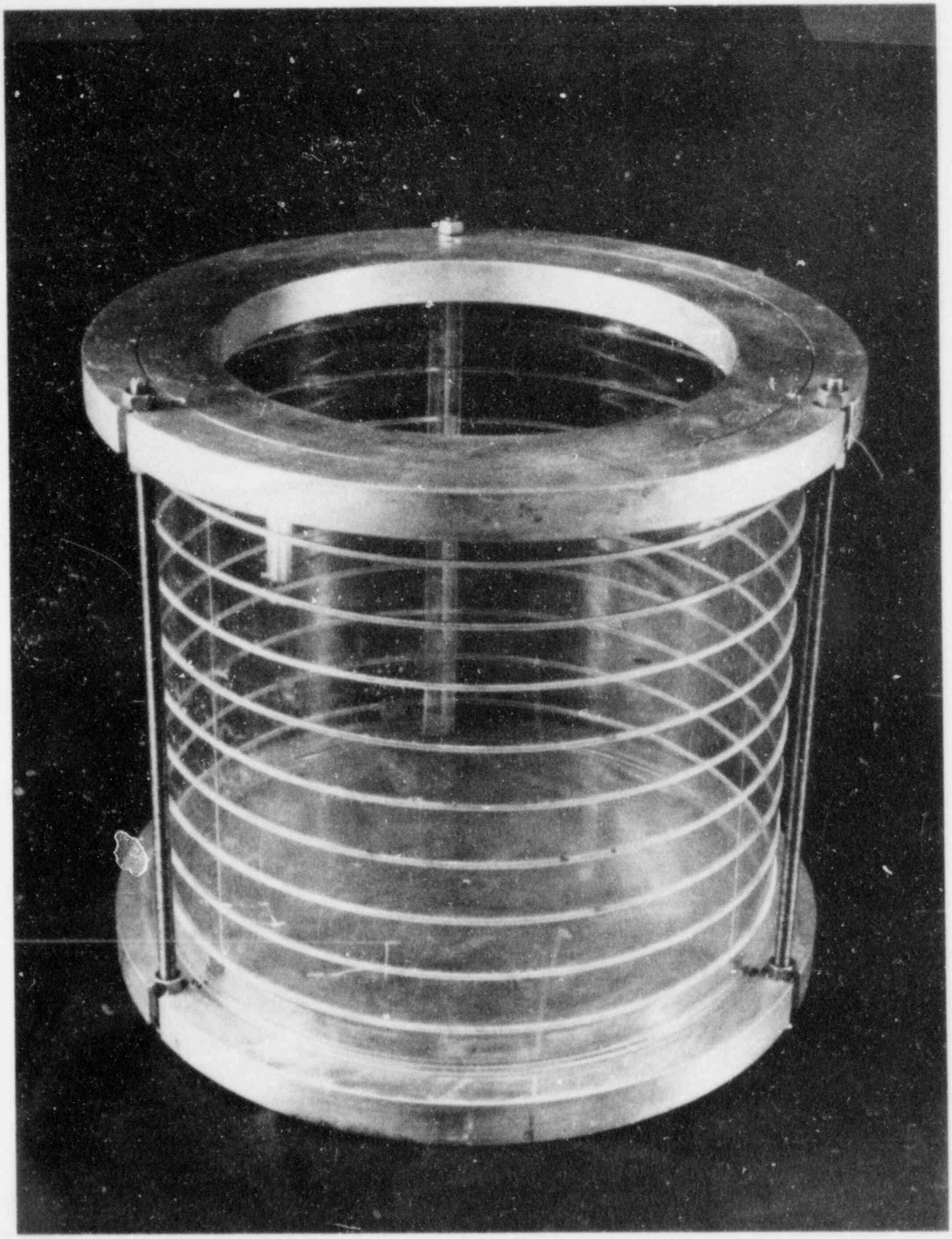

Fig. 6. Ring-stiffened Lexan model.

The time scale, Eq. (11), then becomes

$$N_t = \left[\frac{N_\rho N_\ell}{N_E} \cdot N_\ell\right]^{1/2} = N_\ell \sqrt{\frac{N_\rho}{N_E}} \quad . \tag{17}$$

It is convenient at this time to define the mass scale as

$$N_m = \frac{M_m}{M_p} \quad , \tag{18}$$

where M is any characteristic mass. In terms of the density scale, the mass scale may be written as

$$N_m = N_\rho N_\ell \quad .$$

The distortion of gravity distorts the gravitational forces, and the degree of distortion may be understood by determining the scale factors for the three types of forces acting in the dynamic-buckling problem: gravitational, elastic, and inertial. These scale factors are derived as follows:

Gravitional forces: magnitude $F_g = mg$,

scale $N_{Fg} = N_m N_g$, and

$$N_{Fg} = N_\rho N_\ell^3 \quad (N_g = 1 \text{ during tests}). \tag{19}$$

Elastic forces: magnitude $F_E = \sigma_A$,

scale $N_{FE} = N_\sigma N_\ell^2$, and

$$N_{FE} = N_E N_\ell^2 \quad . \tag{20}$$

Inertial forces: magnitude $F_I = m\ddot{x}$,

scale $N_{FI} = N_m N_{\ddot{x}}$, or

$$N_{FI} = N_E N_\ell^2 \ . \qquad (21)$$

The equations above show that the gravitational forces will be scaled differently from the other important forces. However, the elastic forces and inertial forces have the same scale, and this equivalence is quite important for a continuous system such as this one.

Two sizes of polycarbonate models will be used in this study, 1/50 and 1/100. It is informative to look at the scales associated with these models, and Table I has been prepared for this purpose. A study of this table shows that gravity will be distorted by a factor of 3.83 for the 1/50 scale model; thus, the gravitational forces on the model will be too low by that factor.

E. Steel Models

The models for the bench mark type of tests will be made of steel, specifically A516 Gr 70, a typical structural steel used in containments. Scale models made of the same material as the prototype are commonly called replica models. As mentioned earlier, use of the prototype material in the model will eliminate distortions (and, therefore, problems in interpretation of model results) in the model caused by deformations beyond the proportional limit.

As with the plastic models, a Mark III containment will be used as a basis for the design. Geometrical features to be addressed in the model will include

1. radius-to-wall-thickness ratio,
2. radius-to-height ratio,
3. ring-stiffener geometry area (the section modulus designed to satisfy the ASME code requirements),
4. dome, and
5. equipment access penetrations, with reinforcement designed to satisfy the ASME code requirements.

The variable wall thickness commonly found on containments will not be modeled.

The length scale selected for the replica models is 1/32. The diameter will be slightly larger than the "Base line and Follow-on Bench mark" series

TABLE I

SCALE FACTORS FOR POLYCARBONATE MODELS

Dimensions, Properties	Prototype	Model-Large	Model-Small
Diameter	115 ft	27.5 in.	13.75 in.
Wall Thickness	1.5 in.	0.03 in.	0.015 in.
Height (cylindrical sec.)	115 ft	24.00 in.	12.00 in.
Modulus of Elasticity	29×10^6 psi	0.340×10^6 psi	0.340×10^6 psi
Specific Weight	489 lb/ft^3	74.9 lb/ft^3	74.9 lb/ft^3
Scales			
Length		1/50	1/100
Time		1/13.8	1/27.7
Acceleration		3.83	7.66
Modulus of Elasticity		1/85.3	1/85.3
Density		1/6.53	1/6.53
Force-Gravitional		1/816,000	$1/6.53 \times 10^6$
Elastic		1/213,000	1/853,000
Inertial		1/213,000	1/853,000

of tests reported in Refs. 10 and 11, but the model is of a size that can be easily handled and transported without great difficulty. There will be some benefit accruing from the fact that it is the same scale as one series of steel containment-model tests being conducted by Sandia Laboratories with NRC support.

For this replica model, the elastic modulus scale and density scale are fixed at 1. Once this decision on the material is made, other scale factors can be calculated. The acceleration scale from Eq. (16) becomes

$$N_x = \frac{N_E}{N_\rho N_\ell} = \frac{1}{N_\ell} \quad . \tag{22}$$

This equation shows that, as for the case of the plastic model, distortions will be introduced in the gravity scale as a result of the use of this material. Using Eq. (11) gives the time scale

$$N_t = N_\ell \quad .$$

The force scales for the replica model are determined from Eqs. (19) through (21).

Using the equations developed above, the scale factors for the replica model are calculated and summarized below.

N_ℓ	=	1/32
N_t	=	1/32
$N_{\ddot{x}}$	=	32
N_E	=	1
N_ρ	=	1
N_F Gravitational	=	1/32,700
N_F Elastic	=	1/1024
N_F Inertial	=	1/1024

Use of a replica model of this design, with test conditions and data reduction in accordance with these scale factors, will result in distortion of the gravitational forces by a factor of 32. A preliminary analysis of the effect of this distortion on the buckling problem has been completed. Initial studies show that the axial membrane stresses in typical steel containments will be in the range of 500 psi to 1000 psi. For buckling stresses in the vicinity of 20,000 psi, the gravitational stresses would be 2.5 to 5% of the buckling stresses. This indicates that the static gravitational stresses will not have a significant effect on the results of the model tests.

It should be noted that any distortion effect would not impair the utility of the results for comparison with computer code prediction, because the actual physical model tested would be modeled in the computations. Any noticeable effect of the distortion would show up in indications of actual containment response based upon the model tests. The significance of this distortion will be studied further.

F. Model Experiments

The purpose of the model experiments is to assess the reliability of present methods of predicting dynamic buckling when applied to containment-like structures. This assessment will involve the tasks discussed below.

1. Static-Buckling Allowables. The predominant stresses expected in the transient response of a containment structure are axial compression and shear. The axial stress may result from a bending moment induced by seismic loading or by nonuniform internal pressure on the containment shell. In either case, it is expected that the axial stress will be greatest at the base of the shell. The shear stress will also be expected to have some axial variation that will depend upon both the mass distribution of the containment structure and the loading.

The static test configuration chosen to duplicate the expected stress field is shown in Fig. 7. Interaction results for an unstiffened and a ring-stiffened shell are reported in Ref. 12. This loading condition produces the following stress state in the shell (assuming a membrane state of stress):

$$N_{x\theta} = \frac{S}{\pi R} \sin \theta ,$$

$$N_x = - \frac{S}{\pi R^2} x \cos \theta + \frac{P}{2\pi R} ,$$

where the coordinate system is shown in Fig. 7 and

$S = F \cos \phi$

$P = F \sin \phi$.

By varying the load angle, ϕ, the relative values of shear stress ($N_{x\theta}$) and axial stress (N_x) can be changed. Interaction curves for two shells are shown in Fig. 8 (from Ref. 11). These curves have been normalized using the critical conditions at $\phi = 0^o$ and 90^o. For the data presented in this figure, the stresses were evaluated at $\theta = 90^o$.

The interaction curves for the stiffened and unstiffened shells are much the same when appropriately normalized. The results are not conservative when compared with a recommended interaction curve (Ref. 13), given by

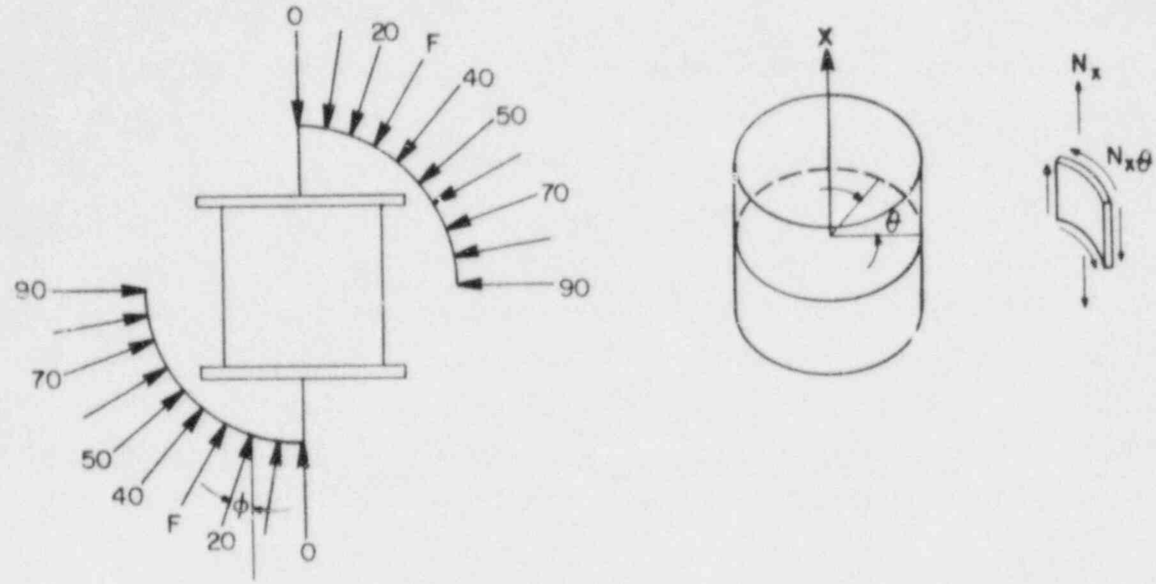

Fig. 7. Static-buckling-test load configuration and coordinate system.

$$\left(\frac{N_{x\theta}}{N_{x\theta_{\phi=90}}}\right)^2 + \left(\frac{N_x}{N_{x_{\phi=0}}}\right) = 1 \quad .$$

The nonconservativeness may result from neglecting the axial stress component caused by the bending. However, the general trend of the data follows the interaction curve fairly well.

Part of the present program will be directed towards a better understanding of the interactive-buckling effects. This understanding can be accomplished by conducting other interaction-buckling experiments such as end shear and bending moment as well as axial load. The necessity for these tests will depend upon the outcome of the analysis task.

2. Modal Testing. The normal modes and natural frequencies of the test shells will be determined experimentally as well as numerically. The purpose of these tests is to determine if an accurate numerical model of the test shells has been created; the same numerical model will be used to determine the dynamic stresses for the buckling phase of the test. Therefore, it is necessary to determine the correspondence between the physical and numerical models.

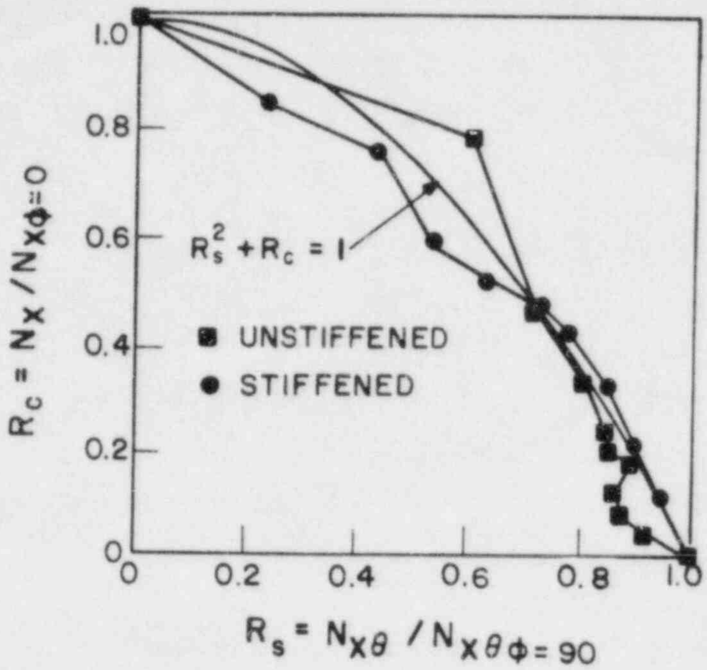

Fig. 8. Interaction-buckling results for shear and compression (Ref. 7).

3. Dynamic Buckling. Dynamic buckling of the model containment structures under seismic loading will be performed using single-axis horizontal base motion, and both harmonic and simulated earthquake base motion. The harmonic testing will increase our understanding of the dynamic-buckling phenomenon under a simple loading.

Harmonic-buckling tests will be conducted by attaching the base ring of the test shell to the slip table of a electromagnetic shaker. Frequency will be set and the amplitude of the base acceleration increased until buckling occurs. Buckling will be detected from shell-wall displacement measurements, by direct observation, and through audible sound.

The analysis task of this program will provide the stresses in the shell wall; these stresses are functions of x, θ, and time. However, for harmonic loading the maximum stresses are easily found because the entire shell vibrates in phase. Using the maximum stress (with respect to x and θ) and the experimentally determined failure criterion, we can predict the critical base acceleration. Comparison with the experimental data provides a direct test of the freezing-in-time analysis procedure.

The harmonic tests can be carried one step further by adding or subtracting mass from the top end ring of the structure. This addition or subtraction has the effect of changing the beam mode frequencies without altering the shell-type frequencies. The ability to change the ratio of response time to buckling time allows an exploration of the range of applicability of the freezing-in-time analysis procedure.

Upon completion of the harmonic-buckling test, seismic response will be investigated. For this test a suitable earthquake will be selected (such as the El Centro record, used in many evaluations) and appropriately time scaled. The test procedure will increase the amplitude of the base motion until buckling occurs. A comparison of this amplitude with buckling analysis prediction gives a measure of analysis reliability. Again, the end mass can be changed to alter the time-scale ratio.

G. Bench Mark Tests

The models to be used for the bench mark tests will be the steel models described earlier in Sec. E. Two models will be constructed for use in two different destructive tests described in the following section.

1. Imperfection Measurements. The imperfections of each model will be measured using the techniques and equipment developed earlier and described in Ref. 10. Imperfection plots will be prepared and data retained for subsequent analysis.

2. Modal Testing. Modal testing will be done to determine, in general, the natural frequencies of several of the shell modes using techniques used for the modal testing of the plastic models. As with the plastic models, the results of these tests will be used as one of the checks on the computer models of the shell that will be developed.

3. Prebuckling Dynamic Tests. The dynamic tests for the bench mark models will be conducted on a single-axis, horizontal shake table. The series of tests will include two types of base motion, harmonic and motion representative of typical seismic activity. The purpose of this series of tests is to collect data on the shell response that may be used to further check the validity of the computer code on steel models. Use of the two types of base motion will allow this to be done for both a steady-state and transient condition. The excitation levels will be well below those required for buckling to occur, and hence, well in the elastic range.

Measurements made during the tests will include the following:

- acceleration vs time for the base,
- acceleration vs time for the bridge crane track location on the model, and
- membrane-strain components at six positions on the shell surface.

A special digital data-acquisition system will be constructed to record the data. The measured strain-time histories will be compared with the predicted strain-time histories from the dynamic analysis for the check.

4. Incipient-Buckling Tests. The incipient-buckling tests will be conducted to determine the mimimum level at which a typical earthquake (horizontal motion only) causes buckling in the model. The base motion will be obtained with a shake table. The first of these tests on a given shell will be run at an earthquake level which is known to be below that required to cause a buckling. Each succeeding test will be at an incrementally higher level. The shell will be inspected and the data studied after each test to determine if buckling has occurred, with permanent deformation as one of the criteria.

Data recorded during this series of tests will be the same as for the prebuckling tests, and in addition, high-speed motion pictures will be taken. One of the models will be expended in this type of test.

5. Postbuckling Behavior. This test will be conducted to determine large postbuckling deformations caused by seismic-like excitation. Once again, base motion will be applied with a horizontal shake table. The level of the representative earthquake will be scaled so that it is well above that required to initiate buckling. The test data recorded will be the same as that mentioned in the previous section, including motion pictures.

This test is expected to provide additional results for correlation of computed and actual g levels required for the initiation of buckling as well as information on postbuckling deformation, which will aid in evaluating the potential for loss-of-containment function from earthquakes.

V. SUMMARY

The combined analytical/experimental program discussed herein will allow a realistic assessment of dynamic-buckling response of steel containments. If the study reveals that the problem of lack of time-scale separation is significant and that dynamic-buckling criteria must be developed, then follow-on efforts will have to be initiated to define the criteria and determine how to derive them. If the current freezing-in-time analysis method is inadequate in certain time loading/response regimes, either full nonlinear dynamic time history analysis will have to be used or methods for accounting for dynamic effects in a simplified manner will have to be developed.

In safety analysis of containments, as pointed out in the intoduction, loading combinations must be evaluated. For example, an extensive freezing-in-time analysis o the Catawba Nuclear Plant was accomplished (Ref. 14). We have specifically addressed seismic loadings only for two reasons: first, there is an obvious overlap in fundamental time scales as we have discussed. Second, seismic loading is fairly easily simulated experimentally for the models used here and will be sufficient to answer most of our questions about current analysis methods. If funding allows, a follow-on effort should probably be initiated to verify the conclusions about load combinations involving LOCA and seismic loadings. However, to carry out an experimental effort on combined loadings without a good understanding of their separate effects would not be productive, and is ill-advised.

Finally, the postbuckling bench mark experiments that are planned should be used by industry to validate nonlinear dynamic computer codes that perform a postbuckling response analysis. This task cannot be undertaken here under the funding as planned, but should be a parallel or follow-on supporting effort. Another very significant problem that must be addressed, if failure margin is to be established, is the quantification of loss of containment by material separation (splitting), rupture or puncture, seal violation, penetration (hardpoint) effects, and the effect of field fabrication. The effort here is limited to the bench mark experimental task that will address postbuckling loss-of-containment potential, but a follow-on or supporting task should address these quantitative failure criteria.

In conclusion, this work plan is designed to resolve the most funadmental issues that are in doubt for buckling of steel containment shells under time-dependent loadings and to further define the needs for future research in this area. Completion of the tasks that have been defined will answer NRC's most pressing needs and will accomplish the objectives of this program.

REFERENCES

1. E. Meller and D. Bushnell, "Buckling of Steel Containment Shells--Task 1A: Dynamic Response and Buckling of Offshore Power Systems Floating Nuclear Plant Containment Vessel," NUREG/CR-2836, LMSC D 812950, Vol. 1, Part 1 (December 1982).

2. "Design Response Spectra For Seismic Design of Nuclear Power Plants," U.S. Atomic Energy Commission Regulatory Guide 1.60, Rev. 1 (December 1973).

3. Choon-Foo Shih, "Failure of Liquid Storage Tanks Due to Earthquake Excitation," Ph.D. thesis, California Institute of Technology, (June 1981).

4. S. Klein, "SABOR/DRASTIC 7 - User's Manual," The SABOR Manual, Vol. III, Poulter Laboratory Technical Report (Stanford Research Institute, Menlo Park, California, 1984).

5. D. Bushnell, "BOSOR 4: Program for Stress, Buckling, and Vibration of Complex Shells of Revolution," in Structural Mechanics Software Series - Vol. 1, N. Perrone and W. Pilkey, Ed. (University Press of Virginia, Charlottesville, Virginia, 1976).

6. D. Bushnell, "Buckling of Elastic-Plastic Shells of Revolution with Discrete Elastic-Plastic Ring Stiffeners," Int. J. Solids and Structures, Vol. 12, pp. 51-56 (1976).

7. W. D. Whetstone, "Spar Structural Analysis System Reference Manual," NASA CR 145098-1 (February 1977).

8. H. D. Hibbitt, B. I. Karlsson, and E. P. Sorenson, ABAQUS-User's Manual, (Hibbitt, Karlsson and Sorenson, Inc., Providence, Rhode Island, 1983).

9. C. D. Babcock, "Experiments in Shell Buckling," Thin Shell Structures - Theory, Experiment and Design, Y. C. Fung and E. E. Sechler, Ed., (Prentice Hall, New York, 1974), pp. 345-369.

10. W. E. Baker, J. G. Bennett, and C. D. Babcock, "Buckling Investigation of Ring-Stiffened Cylindrical Shells Under Unsymmetrical Axial Loads," Los Alamos National Laboratory report LA-9536-MS, NUREG/CR-2966 (October 1982).

11. W. E. Baker and J. G. Bennett, "Buckling Investigation of Ring-Stiffened Cylindrical Shells with Reinforced Openings Under Unsymmetrical Axial Loads," Los Alamos National Laboratory report LA-9646-MS, NUREG/CR-3135 (February 1983).

12. W. E. Baker and J. G. Bennett, "Experimental Investigation of the Buckling of Nuclear Containment-Like Cylindrical Geometries Under Combined Shear and Bending," Los Alamos Scientific Laboratory document LA-UR-83-1771 (submitted to Nuclear Engineering and Design, June 1983).

13. E. H. Baker, A. P. Cappelli, L. Kovalevsky, F. L. Rish, and R. M. Verette, "Shell Analysis Manual," NASA CR 192 (April 1968).

14. A. I. Unsal, N. F. Morris, and G. A. Harstead, "Containment Vessel Stability Analysis Catawba Nuclear Station, Units I and II," Duke Power Co. report 8106-2 (May 27, 1982).

DISTRIBUTION

	Copies
Nuclear Regulatory Commission, R5, Bethesda, Maryland	348
Technical Information Center, Oak Ridge, Tennessee	2
Los Alamos National Laboratory, Los Alamos, New Mexico	50
Total	400

NRC FORM 335
(6 83)

U.S. NUCLEAR REGULATORY COMMISSION

BIBLIOGRAPHIC DATA SHEET

1. REPORT NUMBER (Assigned by TIDC, add Vol. No., if any)
NUREG/CR-3742
LA-10087-MS

2. Leave blank

3. TITLE AND SUBTITLE
Buckling of Steel Containment Shells Under Time-Dependent Loading

4. RECIPIENT'S ACCESSION NUMBER

5. DATE REPORT COMPLETED
MONTH: March
YEAR: 1984

6. AUTHOR(S)
C. D. Babcock, W. E. Baker, J. Fly, J. G. Bennett

7. DATE REPORT ISSUED
MONTH: May
YEAR: 1984

8. PERFORMING ORGANIZATION NAME AND MAILING ADDRESS (Include Zip Code)
Los Alamos National Laboratory
Los Alamos, NM 87545

9. PROJECT/TASK/WORK UNIT NUMBER

10. FIN NUMBER
A7221

11. SPONSORING ORGANIZATION NAME AND MAILING ADDRESS (Include Zip Code)
Division of Engineering Technology
Office of Nuclear Regulatory Research
U.S. Nuclear Regulatory Commission
Washington, DC 20555

12a. TYPE OF REPORT
Informal

12b. PERIOD COVERED (Inclusive dates)

13. SUPPLEMENTARY NOTES

14. ABSTRACT (200 words or less)

The problem of dynamic effects for steel containment shells subjected to time-dependent loadings that produce large compressive membrane stresses in the shell wall is considered. Loadings on typical containment structures are reviewed, along with a description of the complete dynamic-buckling problem. Simplifications and the assumptions that are currently used are critically examined and reviewed with respect to buckling analysis. Based on these reviews, three program objectives are defined and the tasks that can accomplish these objectives within a 2-year effort at level funding are outlined in detail.

15a. KEY WORDS AND DOCUMENT ANALYSIS

15b. DESCRIPTORS

16. AVAILABILITY STATEMENT
Unlimited

17. SECURITY CLASSIFICATION (This report)
Unclassified

18. NUMBER OF PAGES

19. SECURITY CLASSIFICATION (This page)
Unclassified

20. PRICE
$

☆U.S. GOVERNMENT PRINTING OFFICE: 1984-0-776-026/4079

Los Alamos